PAPER

Check for updates

Polynorbornene with silicon cluster pendant groups†

Nhien Q. Nguyen, [ID] [a] Aracely Gonzalez, [ID] [a] Holly N. Lusk,[a] Lan D. Pham [ID] [a] and Timothy A. Su [ID] *[a,b]

Multicyclic oligosilane clusters like permethylated bicyclo[2.2.2]octasilane (Si[2.2.2]) represent a new class of electronic insulators that harness quantum effects (*i.e.*, destructive σ-quantum interference (σ-DQI)) to suppress charge transport. Polymeric insulators that operate from σ-DQI principles are highly promising for applications in ultrathin dielectrics. To realize such applications, however, it is crucial to devise strategies for incorporating molecular silicon clusters into polymeric materials. Here we describe the design, synthesis, and characterization of the first polymers with oligosilane clusters as pendant groups. We first describe our process to find a successful synthetic route to install alkyl-spaced norbornene termini onto Si[2.2.2] clusters. Next, we show these clusters remain structurally intact under ring-opening metathesis polymerization (ROMP) conditions to yield high molecular weight polymers with relatively narrow polydispersity (M_n = 902–1289 kDa, Đ = 1.54–1.68). UV-vis absorbance studies show that the cluster-polymer hybrids retain the same optical absorbance features that are specific to the discrete monomeric cluster. Crucially, we find that installing the Si[2.2.2] cluster pendants to polynorbornene backbones results in emergent improvements in thermal stability, where the decomposition temperature of the cluster-polymer hybrid ($T_d \sim$ 340 °C) increases by 80 °C compared to the free monomer. These results suggest cluster-polymer hybridization is a general strategy to improve the thermal stability of silicon cluster materials. We anticipate that the synthesis and characterization of the silicon cluster-polymer hybrids herein will be a key stepstone toward evaluating silicon clusters as σ-quantum interference-enabled dielectric materials.

Introduction

Electrical insulators play key roles in modern electronics where they are used as dielectrics in capacitors and field-effect transistors, high-voltage insulators, and protective coatings. Their ability to build capacitive charge enables their use in energy harvesting, energy storage, and electronic devices.[1–3] As the demand for ultrathin dielectrics increases,[4–6] it is becoming increasingly critical to find new forms of insulators that are even more resistive than what is presently used.

Multicyclic oligosilane clusters, particularly the permethylated bicyclo[2.2.2]octasilane (Si[2.2.2]) motif,[7–9] are highly promising molecular materials in this regard. In 2018, the charge transport properties of Si[2.2.2] clusters with gold-binding methylthiomethyl endgroups (Fig. 1a) were interro-

gated in single-molecule junctions with the scanning tunneling microscopy break-junction (STM-BJ) technique.[10] This study revealed that the *cis*-like dihedrals of the constrained oligosilane bridges invert the symmetry and energetic ordering of the frontier molecular orbitals (MOs) that are critical for charge transport. These inversions caused strong destructive σ-quantum interference (σ-DQI) to occur between the transmitting MO channels, leading to molecular junctions that are even more electrically resistive than vacuum gaps of the same length. Solomon and coworkers invoked interatomic transmission pathway calculations[11] to show that significant ring current reversal effects (Fig. 1a) arise from σ-DQI. Notably, Si[2.2.2] clusters were found to be far more resistive on a per-length basis than the canonical alkane and siloxane insulators that are molecular analogs of bulk scale polymeric insulators like polypropylene and silicon dioxide, and more resistive than π-conjugated DQI insulators.[12–14] These studies pointed to Si[2.2.2] clusters as potential next-generation insulators where ultrahigh resistance may be achieved through destructive σ-quantum interference effects.

Towards realizing this vision, it becomes necessary to consider how to incorporate Si[2.2.2] structures into soft

[a]Department of Chemistry, University of California, Riverside, CA, USA.
E-mail: timothys@ucr.edu
[b]Materials Science and Engineering Program, University of California, Riverside, CA, USA

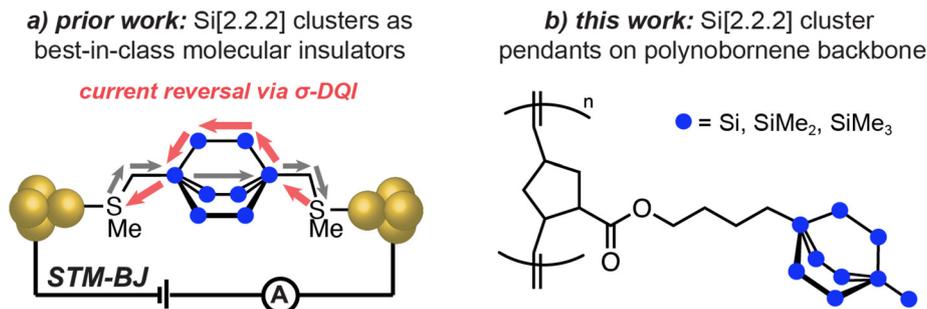†Electronic supplementary information (ESI) available. See DOI: https://doi.org/10.1039/d5py00465a

Fig. 1 (a) Schematic of prior scanning tunneling microscopy break-junction (STM-BJ) studies on single-molecule junctions of Si[2.2.2] clusters with methylthiomethyl endgroups attached between gold electrodes (gold spheres). These clusters were found to be even more insulating than vacuum gaps of the same dimensions due to destructive σ-quantum interference (σ-DQI) effects. The arrows summarize calculated interatomic transmission pathways with forward current (gray arrows) and reverse current (red arrows) flow as a graphical representation for transport annulment across the molecular junction. These prior studies motivate the present work to explore polymers built from σ-DQI concepts. (b) This work describes the synthesis and characterization of the first polymers incorporating the Si[2.2.2] building block.

materials, as molecular clusters lack the flexibility, processability, and film robustness of polymers. Indeed, cluster-polymer hybrid materials have been devised for metallic,[15–18] metal chalcogenide,[19] metal-oxo,[20–22] silsesquioxane,[23–26] borane,[27] carborane,[28–30] phosphorous-nitrogen cages,[31–35] and other[36–38] clusters to achieve properties and functionalities that are often greater than the sum of their parts. These studies motivated us to explore whether we could similarly access Si[2.2.2] cluster-polymer hybrids (Fig. 1b). Polysilanes[39,40] and polymers with cyclosilane subunits[41–45] are known. Hybrid polynorbornenes with silane[46–53] and siloxane subunits[25,46,54–57] are also known. But there are no examples to our knowledge of polymeric structures with multi-cyclic silicon cluster building blocks.

Here we enact ring-opening metathesis polymerization (ROMP) on a norbornene-terminated Si[2.2.2] monomer to access the first polymers with multicyclic silicon cluster pendant groups. Nuclear magnetic resonance (NMR) studies reveal the oligosilane clusters remain intact under ROMP conditions. UV-vis absorbance studies show that the polymer retains the optical absorbance features intrinsic to the free cluster. Meanwhile, thermogravimetric analysis studies show that Si[2.2.2] clusters become significantly more robust to thermal degradation when affixed to polynorbornene backbones compared to the free cluster molecule, a result that suggests polymer attachment\is a general strategy to increase the thermal stability of silicon clusters. The synthesis and characterization of silicon cluster-polymer hybrid materials reported herein paves a path to exploring their use as dielectric materials.

Experimental

Materials and characterization methods

Unless otherwise specified, all chemicals were used as purchased without further purification. Solvents used for recrystallization, column chromatography and polymer workup were reagent grade and used as received. Reaction solvents toluene, tetrahydrofuran (THF), dichloromethane (DCM) were dried and degassed on a J. C. Meyer solvent dispensing system following the manufacturer's recommendations for solvent preparation and dispensation.

Materials. Potassium *tert*-butoxide (KO^{t}Bu, 97%) was purchased from Alfa Aesar. 18-crown-6 (18-C-6, >99%) was purchased from Oakwood Chemical. 1,2-Dichlorotetramethyldisilane (95%) was purchased from Gelest. 1-Bromo-4-(*t*-butyldimethylsilyloxy)butane (98%) was purchased from Combi-Blocks. Acetyl chloride (AcCl, >98%) was purchased from TCI America. Anhydrous methanol (MeOH, 99.90%) was purchased from Fisher Scientific. *N,N*'-Dicyclohexylcarbodiimide (DCC, 99%) and ethyl vinyl ether (stabilized with KOH, 98%) were purchased from AK Scientific. 4-(Dimethylamino)pyridine (DMAP, ≥±99%), *exo*-5-norbornenecarboxylic acid (Nb-COOH, 97%) and Grubbs 2nd generation catalyst were purchased from Sigma-Aldrich. Differential scanning calorimetry (DSC) and thermal gravimetric analysis (TGA) crucibles were purchased from Netzsch.

Instrumentation and measurements. ^{1}H NMR, ^{13}C NMR, and ^{29}Si DEPT NMR were recorded on Bruker NEO400 (400 MHz) and Bruker AV 600 (600 MHz) spectrometers. Chemical shifts for ^{1}H NMR are reported and referenced to residual protium in NMR solvents (CHCl$_3$, δ 7.26). Chemical shifts for ^{13}C NMR are reported in parts per million downfield from tetramethylsilane and are referenced to the center peaks of residual solvents (CHCl$_3$, δ 77.16). Chemical shifts for ^{29}Si are reported in parts per million downfield from tetramethylsilane and are referenced to a tetramethylsilane external standard. To compensate for the low isotopic abundance of ^{29}Si, the DEPT pulse sequence was employed for the amplification of the signal. Data are represented as follows: chemical shift, multiplicity (s = singlet, d = doublet, t = triplet, q = quartet, m = multiplet), coupling constants in Hertz, and integration.

For molecular mass characterization, low-resolution mass spectrometry (LRMS) was recorded on a Waters XEVO G3 QToF mass spectrometer equipped with a UPC2 SFC inlet, electro-

spray ionization (ESI) probe, atmospheric pressure chemical ionization (APCI) probe, and atmospheric solids analysis probe (ASAP).

For polymer mass characterization, the absolute molecular weights (M_w, M_n) and polydispersity index (PDI) of the polymers were determined using size exclusion chromatography coupled with multi-angle light scattering (SEC-MALS). A miniDawn TREOS MALS detector and Optilab dRI refractive index detector, both from Wyatt Technology, were employed as the primary detectors. THF was used as the mobile phase. Injections were carried out using a Shimadzu LC-2050 HPLC system, with a flow rate of 1 mL min^{-1} over 20 minutes, and injection volumes of 20 μL to avoid detector saturation due to the high molecular weight of the samples. Supplemental concentration detection was performed using a UV channel at 254 nm. Polystyrene standards with molecular weights of 29 kDa and 128 kDa were used for calibration, allowing for the normalization of the three scattering angles of the MALS detector. Detector alignment and chromatogram correction (including band broadening) were applied to ensure accurate data processing. The refractive index increment (dn/dc) for each sample was determined using Wyatt's ASTRA software. The dn/dc values were calculated based on a 100% mass recovery method, ensuring accurate quantification of polymer concentration during the analysis.

Powder X-ray diffraction (PXRD) analysis was performed using Empyrean PANalytical Series 2 system with a Cu-Kα source (λ = 1.541 Å) to characterize **1** and **PNB-Si[2.2.2]**. The materials were ground into a fine powder and analyzed using a zero-diffraction plate (32 mm diameter × 2.0 mm thickness, Si crystal) purchased from MTI Corporation. Thermogravimetric Analysis (TGA) curves were obtained from ∼1–2 mg of sample in an alumina crucible (6 m, 25/40 μl) and analyzed by Netzsch TG 209 F1 Libra from 25 °C to 600 °C under N$_2$ atmosphere with a heating rate of 10 °C min^{-1}. Differential Scanning Calorimetry (DSC) was carried out using a Netzsch 214 Polyma DSC. Samples (1–2 mg) were sealed in aluminum concavus crucibles (6 mm; 25/40 μL). Heat-cool-heat cycles from −30 °C to 320 °C were performed with both heating and cooling rates of 10, 20, 30 °C min^{-1} under N$_2$ (Fig. S1 and S2†). Ultraviolet-visible (UV-vis) absorbance spectra were collected with an Aglient Cary 60 UV-Vis Spectrophotometer, with samples made in spectroscopy-grade cyclohexane (Uvasol) in a 1 cm quartz cuvette.

Synthesis of 3

An oven-dried 250 mL Schlenk flask with a stir bar was charged with **1** (3.92 g, 7.11 mmol, 1.0 equiv.), potassium *tert*-butoxide (0.79 g, 7.11 mmol, 1.0 equiv.), 18-crown-6 (1.88 g, 7.11 mmol, 1.0 equiv.) and dissolved in dry toluene (60 mL). The reaction was stirred at room temperature overnight under nitrogen. The reaction mixture was cooled to −78 °C with a dry ice-acetone bath, upon which 1-bromo-4-(*t*-butyldimethylsilyloxy)butane (1.90 g, 7.11 mmol, 1.0 equiv.) was added dropwise into the mixture. After addition, the dry ice bath was removed, and the reaction was stirred at room temperature for

2 h. The solution changed from orange to colorless as it slowly warmed to room temperature. The reaction mixture was quenched with deionized water (15 mL). The aqueous layer was extracted with anhydrous diethyl ether (3 × 15 mL) and the combined organic layers were brine-washed, dried over sodium sulfate, then concentrated *in vacuo* yielding the crude material as an off-white semi solid (4.87 g). The crude material was used without further purification, as higher yields were obtained over a two-step sequence this way.

^{1}H NMR (600 MHz, CDCl$_3$)	δ 3.61 (dt, J = 6.2, 3.4 Hz, 2H), 1.59–1.52 (m, 2H), 1.52–1.45 (m, 2H), 0.89 (s, Hz, 9H), 0.27 (s, 18H), 0.25 (s, 18H), 0.22 (s, 9H), 0.04 (s, 6H).
^{13}C NMR (151 MHz, C$_6$D$_6$)	δ 65.00, 39.90, 28.58, 20.88, 10.61, 6.15, 2.36, 1.35, −2.77.
^{29}Si NMR (79 MHz, CDCl$_3$)	δ 18.27, −5.85, −38.02, −40.50, −76.67, −130.30.

LRMS (ASAP) for [C$_{25}$H$_{68}$OSi$_{10}$]: calculated = 664.3, found = 665.2 [M + H]$^+$

Synthesis of 4

Synthesis of **4** was modified from Khan *et al.*:[58] an oven-dried 100 mL RBF with a stir bar was charged with **3** (1.5 g, 2.25 mmol, 1.0 equiv.) and dissolved in dry THF (10 mL). Acetyl chloride (0.801 mL, 11.27 mmol, 5.0 equiv.) and methanol (0.456 mL, 11.27 mmol, 5.0 equiv.) were added at 0 °C over an ice bath. The ice bath was removed after addition of reagents, and the reaction was stirred at room temperature under nitrogen for 1 hour. The reaction mixture was quenched with deionized water (5 mL). The aqueous layer was extracted with anhydrous diethyl ether (3 × 15 mL) and the combined organic layers were brine-washed, dried over sodium sulfate, then concentrated *in vacuo*. The product was purified *via* silica gel chromatography by using 10% ethyl acetate in hexanes as eluent to yield **4** as a white solid (0.48 g, 40% yield).

^{1}H NMR (600 MHz, CDCl$_3$)	δ 3.65 (q, J = 6.1 Hz, 2H), 1.62 (p, J = 6.7 Hz, 2H), 1.53–1.45 (m, 2H), 1.15 (t, J = 5.4 Hz, 2H), 0.96–0.89 (m, 2H), 0.28 (s, 18H), 0.25 (s, 18H), 0.23 (s, 9H).
^{13}C NMR (101 MHz, CDCl$_3$)	δ 62.58, 37.10, 25.35, 7.86, 3.55, −1.32, −2.63.
^{29}Si NMR (119 MHz, CDCl$_3$)	δ −5.83, −38.05, −40.51, −76.63, −130.43.

LRMS (ASAP) for [C$_{19}$H$_{54}$OSi$_9$]: calculated = 550.2, found = 551.1 [M + H]$^+$

Synthesis of 5

An oven-dried 100 mL Schlenk flask with a stir bar was charged with *exo*-5-norbornene carboxylic acid (0.17 g, 1.20 mmol, 1.0 equiv.), *N,N′*-dicyclohexylcarbodiimide (DCC, 0.38 g, 1.80 mmol, 1.5 equiv.), 4-dimethylaminopyridine (4-DMAP, 0.015 g, 0.12 mmol, 0.1 equiv.), **4** (0.73 g, 1.32 mmol, 1.1 equiv.) and dissolved in dry DCM (15 mL). The byproduct formed was filtered over a fritted funnel after the reaction completed. Aqueous workup was carried out with NaHCO$_3$ (10 mL). The aqueous layer was extracted with DCM (3 × 15 mL) and the combined organic layers were brine-washed, dried over magnesium sulfate, then concentrated *in vacuo*. The product was purified *via* silica gel chromatography by using

30% DCM in hexanes as eluent to yield **5** as a white solid (0.63 g, 78% yield).

^{1}H NMR (600 MHz, CDCl$_3$)	δ 6.12 (dt, J = 19.3, 5.0 Hz, 2H), 4.10 (t, J = 6.5 Hz, 2H), 3.03 (s, 1H), 2.92 (s, 1H), 2.21 (dd, J = 9.9, 4.3 Hz, 1H), 1.92 (ddz, J = 12.3 Hz, 1H), 1.68 (p, J = 6.9 Hz, 2H), 1.58–1.45 (m, 3H), 1.39–1.32 (m, 2H), 0.96–0.90 (m, 2H), 0.28 (s, 18H), 0.25 (s, 18H), 0.23 (s, 9H).
^{13}C NMR (101 MHz, CDCl$_3$)	δ 176.32, 138.02, 135.80, 64.02, 46.65, 46.42, 43.27, 41.64, 32.86, 30.33, 25.71, 7.70, 3.55, −1.33, −2.65.
^{29}Si NMR (79 MHz, CDCl$_3$)	δ −5.82, −38.04, −40.51, −76.48.

LRMS (ASAP) for [C$_{27}$H$_{62}$O$_2$Si$_9$]: calculated = 670.3, found = 671.2 [M + H]$^+$

Polymerization of 5 to PNB-Si[2.2.2]

Each polymerization was carried out with the same general protocol. Synthesis of entry 3 (M : I = 2000 : 1) from Table 1 is provided here as an example. **5** (100 mg, 0.149 mmol, 2000 equiv.) was weighed out into a 20 mL vial equipped with a stir bar, then transferred into the glovebox and diluted with 4 mL DCM. A stock solution of Grubbs-2 catalyst (5.0 mg (weighed out with an ultramicrobalance) in 0.625 mL DCM) was also prepared inside the glovebox. 7.90 μL of this stock solution (0.0745 μmol, 1.0 equiv.) was added to a solution of **5** at room temperature and allowed to stir for 1 hour. 1.0 mL of ethyl vinyl ether was used to quench the polymerization. Excess ethyl vinyl ether was removed *in vacuo*. The crude polymer was dissolved in 2 mL of anhydrous DCM and added dropwise into 40 mL of stirring methanol, forming a white precipitate. The resulting polymer was isolated from the filtrate filtration with a 0.45 μm membrane filter, then dried in a vacuum oven at 75 °C to yield the polymer (0.0821 g, 82% yield). The ^{1}H, ^{13}C, and ^{29}Si-DEPT NMR spectra are provided in Fig. 2 as well as the ESI.†

Polymerization of *exo-n*-butyl 5-norbornene-2-carboxylate to PNB-C

exo-n-Butyl 5-norbornene-2-carboxylate was synthesized according to Gumbley *et al.*[59] The polymer was synthesized with a 500 : 1 *M : I* ratio. *exo-n*-Butyl 5-norbornene-2-carboxylate (165 mg, 0.849 mmol, 500 equiv.) was weighed out into a
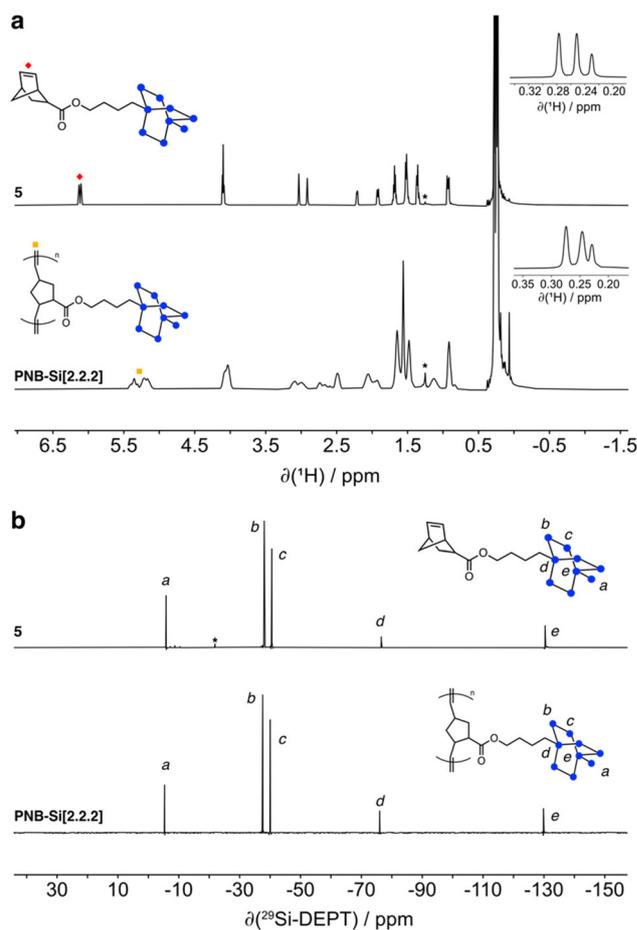
Table 1 Relationship between monomer : initiator ratio and **PNB-Si [2.2.2]** characteristics

Entry	$[M]_0/[I]^a$	Yield^b (%)	M_n^c (kg mol^{-1})	M_w^c (kg mol^{-1})	M_w/M_n^c	DP^d
1	100 : 1	86	902.3	1407	1.56	1343
2	500 : 1	64	1032	1740	1.68	1536
3	2000 : 1	82	1289	1991	1.54	1919

^{a} Molar ratio of monomer **5** to Grubbs G2, with reactions conducted at room temperature with monomer concentration of 0.037 M in dichloromethane, stirring for one hour. ^{b} Isolated product yield. ^{c} Determined by SEC relative to 128 kDa polystyrene standard (THF, [**PNB-Si[2.2.2]**] = 10 mg mL^{-1}, 1 mL min^{-1}, 20 μL injection). ^{d} Degree of polymerization (DP), determined by dividing the M_n (Da) value obtained by SEC for repeating unit mass (RU = 671.61 g mol^{-1}).

Fig. 2 (a) ^{1}H NMR spectra in CDCl$_3$ of monomer **5** and **PNB-Si[2.2.2]**. (b) ^{29}Si-DEPT NMR spectra in CDCl$_3$ of monomer **5** and **PNB-Si[2.2.2]**. Asterisks denote silicone grease peaks.

20 mL vial equipped with a stir bar, then transferred into the glovebox and diluted with 4 mL DCM. A stock solution of Grubbs-2 catalyst (5.0 mg in 0.625 mL DCM, weighed out with a microbalance) was also prepared inside the glovebox. 0.180 mL of this stock solution (1.70 μmol, 1.0 equiv.) was added to a solution of **7** at room temperature and allowed to stir for 1 hour. 1.0 mL of ethyl vinyl ether was used to quench the polymerization. Excess ethyl vinyl ether was removed *in vacuo*. The crude polymer was dissolved in 2 mL of anhydrous DCM and added dropwise into 40 mL of stirring methanol, forming floating white precipitate. The resulting polymer isolated from the filtrate filtration with a 0.45 μm membrane filter, then dried in a vacuum over at 75 °C to yield the polymer (0.089 g, 90% yield). The ^{1}H and ^{13}C NMR spectra matched the previous report in Gumbley *et al.*[59]

Results and discussion

Several approaches exist for the synthesis of polysilanes,[39,42] but many bear reactivity challenges that render them incompa-

tible with cyclic and multicyclic oligosilane monomers. Under Wurtz coupling conditions, alkali metal reduction of permethylated cyclooligosilanes may initiate ring-contraction and redistribution processes.[60] Anionic polymerization conditions are unsuitable, as even weak alkoxide anions can attack and cleave Si–Si bonds or ring-open cyclosilanes.[8,61,62] Promisingly, Klausen and Kawakami have shown Si–Si σ-bonds remain intact under metathesis polymerization conditions.[46,63,64] This prior work suggests that ROMP could be a viable approach for polymers containing silicon cluster building blocks, which inspired us to target polynorbornene backbones with Si[2.2.2] cluster pendants.

Saturated oligosilane clusters are sterically bulky; we thus designed our monomer so an alkane tether separates the large cluster from the reactive norbornene site. We first prepared the known bis-trimethylsilyl-terminated Si[2.2.2] cluster **1** on multigram scale over four steps from commercial reagents, from which we could generate the nucleophilic cluster silanide **2** *via* trimethylsilyl cleavage *via* potassium *tert*-butoxide (Scheme 1).[8] As the compatibility of oligosilyl anions with organic functional groups is not well-charted relative to carbanions, we first screened approaches for installing alkyl-linked norbornenes onto silanide **2**. As we show in Scheme S1,† cluster silanide nucleophiles are incompatible with norbornene double bonds as well as organic azides. Scheme 1 shows our most fruitful approach, where we access the novel norbornene monomer **5** with a bicyclo[2.2.2]octasilane pendant group in three steps from **1** (see ESI† for more details). We first generate **2** from the potassium *tert*-butoxide-mediated cleavage of a terminal trimethylsilyl group in **1**. We then add 1-bromo-4-(*t*-butyldimethylsilyloxy)butane in the same pot to access silyl ether **3**. We remove the *tert*-butyldimethylsilyl protecting group *via* acetyl chloride to give alcohol **4**.[58] Steglich esterification of *exo*-5-norbornenecarboxylic acid with **4** furnishes monomer **5** in a 31% overall yield from **1**.

Next, we used Grubbs G2 catalyst for the ring-opening metathesis polymerization of **5** in dichloromethane to give **PNB-Si [2.2.2]**. Conversion was determined to be complete within an hour, after which the reaction was quenched with ethyl vinyl ether and the polymer precipitated in methanol. ^{1}H NMR analysis shows characteristic signal broadening in the polymer compared to the monomer, accompanied by disappearance of the endocyclic ethenyl proton resonances at ∼6.2 ppm (Fig. 2a) and emergence of the exocyclic ethenyl proton resonances between 5.1–5.5 ppm. The inset of Fig. 2a supports that the Si [2.2.2] cage remains intact with this polymerization approach, as we find the same 2 : 2 : 1 integration ratio of cluster silamethyl proton resonances in both the monomer and polymer ^{1}H NMR spectra. Fig. 2b plots the ^{29}Si-DEPT NMR spectra of **5** and **PNB-Si[2.2.2]** and shows there is essentially no change in [29]Si peak position between monomer and polymer, further supporting that the Si cluster remains intact after ROMP. Table 1 depicts how the monomer:initiator ratio may be controlled to tune polymer size. Larger monomer equivalences allow us to obtain polymers of increasing molecular weight (M_n = 902–1289 kDa) while maintaining narrow polydispersity indices (PDI = 1.54–1.68). While the percent yields are roughly the same for entries 1 and 3 (82–86% yield), it is slightly lower for entry 2 (64% yield), which we speculate arises from experimental variance in the synthesis and workup steps.

With **PNB-Si[2.2.2]** in hand, we sought to address two questions: (1) How do Si cluster pendants impact the physical properties of polynorbornene backbones? (2) How does the behavior of Si[2.2.2] clusters deviate between its polymer-bound and free molecule forms?

To address these questions, we evaluated the structural, thermal, and optical properties of **PNB-Si[2.2.2]** against those of free molecule Si[2.2.2] clusters **1** and **5**, as well as a polynorborene control polymer **PNB-C** (Fig. 3)[59] with *n*-butyl ester side-chains that is structurally similar to **PNB-Si[2.2.2]** but lacks the
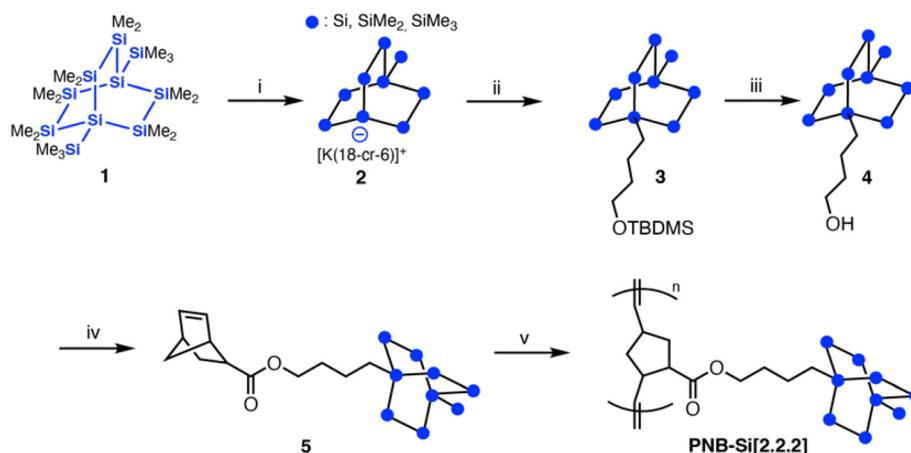
Scheme 1 Synthetic route to monomer **5** and **PNB-Si[2.2.2]** *via* ROMP. (i) Potassium *tert*-butoxide, 18-crown-6, toluene; (ii) 1-bromo-4-(*t*-butyldimethylsilyloxy)butane, −78 °C. (iii) acetyl chloride, methanol, tetrahydrofuran, 0 °C, 40% yield over two steps; (iv) *N,N′*-dicyclohexylcarbodiimide, 4-dimethylaminopyridine, *exo*-5-norbornenecarboxylic acid, dichloromethane, 78% yield; (v) Grubbs G2, dichloromethane, room temperature (see Table 1).
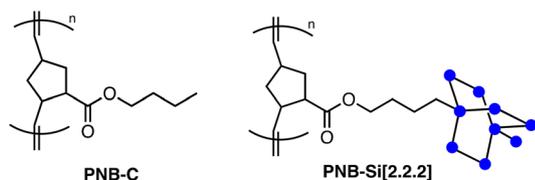
Fig. 3 Chemical structure of **PNB-C**, a control polymer that is structurally similar to **PNB-Si[2.2.2]** but lacks a terminal Si[2.2.2] pendant group.
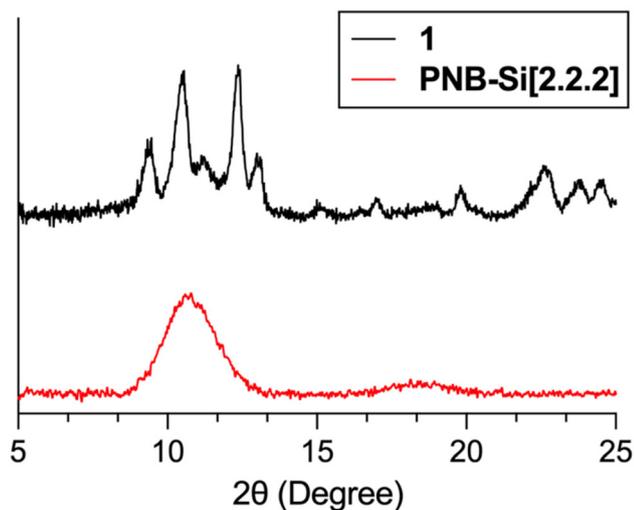

Fig. 4 Powder X-ray diffraction spectrum of **1** and **PNB-Si[2.2.2]** powders.

Si[2.2.2] pendant. We synthesized **PNB-C** using a similar ROMP approach as for **PNB-Si[2.2.2]** (Table S1†).

First, we find that inclusion of the rigid oligosilane cluster along the polynorbornene backbone solidifies the polymer. Whereas **PNB-C** is a colorless gel, **PNB-Si[2.2.2]** is a white solid. We characterize **PNB-Si[2.2.2]** powders as structurally amorphous based on its powder X-ray diffraction pattern (Fig. 4). Comparison against a polycrystalline powder of **1** shows that the sharp peaks that occur between $2\theta = 8°–14°$ are lost in the PXRD spectrum of amorphous **PNB-Si[2.2.2]** that shows broad, undefined peaks. This difference suggests it is more challenging for the pendant Si[2.2.2] clusters to access well-defined long-range ordering interactions when bound to the polynorbornene backbone compared to the free cluster molecule. Next, we explored the thermal stability of **PNB-Si[2.2.2]** compared to **PNB-C** *via* thermogravimetric analysis (TGA). The TGA curve in Fig. 5 shows the onset of thermal decomposition (T_d) in **PNB-Si[2.2.2]** occurs at 340 °C with 5% weight loss, which is 44 °C lower than that of PNB-C ($T_d = 384$ °C). The reduced thermal stability of **PNB-Si[2.2.2]** compared to **PNB-C** suggests the bicyclo[2.2.2]octasilane clusters are the first substructures to degrade within the polymer. This T_d value is close to those of polysilanes with main chain Si–Si σ-bonds where values between 210 °C to 320 °C are commonly reported.[39,44,65,66] Notably, Fig. 5 shows that monomer **5** ($T_d = 260$ °C) decomposes 80 °C lower in temperature than **PNB-Si[2.2.2]**, which indicates that the thermal stability of **Si[2.2.2]** increases significantly when it is bound to the organic polymer backbone rather than in its free form. We conducted DSC measurements from −30 °C to 320 °C under nitrogen and found a weak glass transition (T_g) feature for **PNB-Si[2.2.2]** at 116 °C (Fig. S1 and S2†), which is close in value to previous reports of polynorbornenes with pendant disilane ($T_g \sim$ 120 °C)[46] and trimethylsilane ($T_g \sim$ 113 °C)[67] groups.

Finally, solution-state UV-vis spectra of monomer **5**, **PNB-Si[2.2.2]**, and **PNB-C** in cyclohexane at room temperature show that both **5** and **PNB-Si[2.2.2]** exhibit a strong absorbance feature at 233 nm (Fig. 6), which is consistent with the energies of σ-π*-like optical transitions previously reported for Si[2.2.2] clusters.[68,69] The similar λ_{max} position between **5** and **PNB-Si[2.2.2]** indicates the Si clusters remain electronically iso-
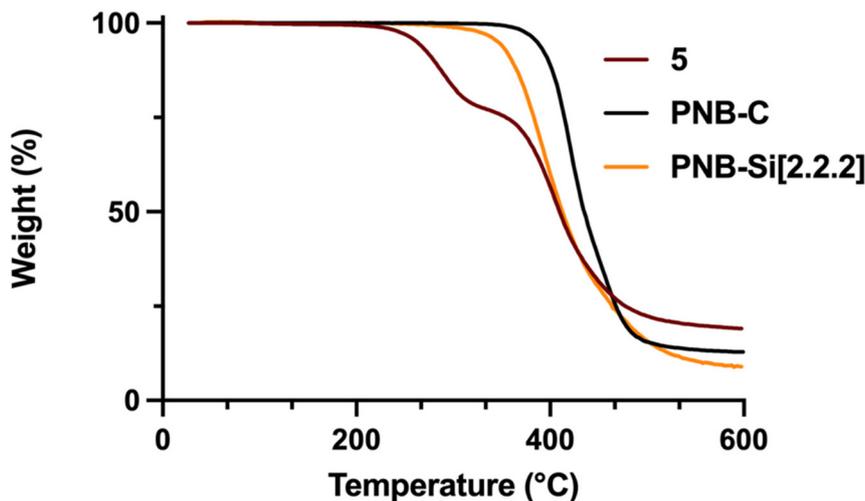

Fig. 5 TGA curves of monomer **5** (dark red line), **PNB-C** (black line) and **PNB-Si[2.2.2]** (orange line) heated under inert nitrogen atmosphere. Heating rate: 10 °C min^{-1}.
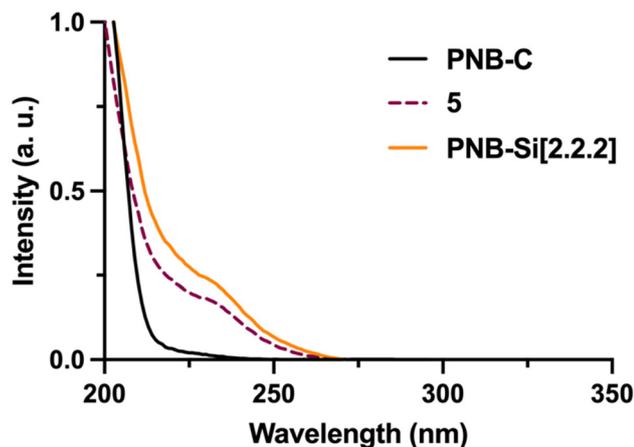
Fig. 6 UV-Vis absorbance spectroscopy of **PNB-C** (black line), **5** (dark red line), and **PNB-Si[2.2.2]** (orange line) in cyclohexane at room temperature. Solution concentrations: [**PNB-C**] = 0.082 mg mL^{-1}, [**5**] = 10 μM, [**PNB-Si[2.2.2]**] = 0.011 mg mL^{-1}.

lated as pendants along the polynorbornene backbone and remains a wide band gap polymer (Fig. 6).

Conclusion

In this work, we outline a general approach to attach norbornene termini to saturated oligosilane clusters. The norbornene functionalization approach revealed for Si[2.2.2] in Scheme 1 should similarly apply to the many multicyclic oligosilane clusters with trimethylsilyl endgroups that exist and can be readily converted to cluster silanides similar to **2**.[70] We thus anticipate that a much broader scope of polynorbornenes with diverse silicon cluster pendants can be realized with the ROMP approach we show here, some of which may be promising future candidates as Si-rich preceramic polymers for hypersonic applications.[71]

Additionally, our TGA studies show that covalently tethering silicon clusters to organic backbones significantly increases its T_d compared to the free cluster, suggesting that polymer attachment may be a generalizable strategy for improving the thermal stability of functional silicon cluster materials. The improved thermal stability of **PNB-Si[2.2.2]** may find relevance for high temperature (>300 °C) dielectric applications such as capacitive energy storage in geothermal, electric aircraft, and space exploration contexts.[72–74] Finally, our UV-vis studies reveal that the characteristic optical features from the discrete cluster are retained in the cluster-polymer hybrid. It is the same set of molecular orbitals that give rise to the optical transitions in Si[2.2.2] that also underlie the strong σ-DQI observed when measuring charge transport across Si[2.2.2]-based single-molecule junctions. This commonality suggests the electrical insulation properties we observe in single molecules should also extend to the cluster-polymer hybrid, and may give rise to new forms of polymeric insulators that operate from destructive quantum interference effects. With **PNB-Si[2.2.2]** in

hand, we are now eager to explore the extent to which destructive σ-quantum interference, a concept first discovered in molecular scale electronics, extends to the design of dielectric materials.

Conflicts of interest

There are no conflicts to declare.

Data availability

The data supporting this article have been included as part of the ESI.†

Acknowledgements

References

1 Y. Qiao, X. Yin, T. Zhu, H. Li and C. Tang, *Prog. Polym. Sci.*, 2018, **80**, 153–162.

2 B. Wang, W. Huang, L. Chi, M. Al-Hashimi, T. J. Marks and A. Facchetti, *Chem. Rev.*, 2018, **118**, 5690–5754.

3 W. Volksen, R. D. Miller and G. Dubois, *Chem. Rev.*, 2010, **110**, 56–110.

4 F. Palumbo, C. Wen, S. Lombardo, S. Pazos, F. Aguirre, M. Eizenberg, F. Hui and M. Lanza, *Adv. Funct. Mater.*, 2020, **30**, 1900657.

5 M. Jenkins, D. Z. Austin, J. F. Conley, J. Fan, C. H. de Groot, L. Jiang, Y. Fan, R. Ali, G. Ghosh, M. Orlowski and S. W. King, *ECS J. Solid State Sci. Technol.*, 2019, **8**, N159.

6 Q.-K. Feng, S.-L. Zhong, J.-Y. Pei, Y. Zhao, D.-L. Zhang, D.-F. Liu, Y.-X. Zhang and Z.-M. Dang, *Chem. Rev.*, 2022, **122**, 3820–3878.

7 A. Indriksons and R. West, *J. Am. Chem. Soc.*, 1970, **92**, 6704–6705.

8 R. Fischer, T. Konopa, S. Ully, J. Baumgartner and C. Marschner, *J. Organomet. Chem.*, 2003, **685**, 79–92.

9 W. Setaka, N. Hamada and M. Kira, *Chem. Lett.*, 2004, **33**, 626–627.

10 M. H. Garner, H. Li, Y. Chen, T. A. Su, Z. Shangguan, D. W. Paley, T. Liu, F. Ng, H. Li, S. Xiao, C. Nuckolls, L. Venkataraman and G. C. Solomon, *Nature*, 2018, **558**, 416–419.

11 G. C. Solomon, C. Herrmann, T. Hansen, V. Mujica and M. A. Ratner, *Nat. Chem.*, 2010, **2**, 223–228.

12 J. P. Bergfield, H. M. Heitzer, C. Van Dyck, T. J. Marks and M. A. Ratner, *ACS Nano*, 2015, **9**, 6412–6418.

13 H. M. Heitzer, T. J. Marks and M. A. Ratner, *J. Am. Chem. Soc.*, 2013, **135**, 9753–9759.

14 H. M. Heitzer, T. J. Marks and M. A. Ratner, *ACS Nano*, 2014, **8**, 12587–12600.

15 W. Y. Chan, S. B. Clendenning, A. Berenbaum, A. J. Lough, S. Aouba, H. E. Ruda and I. Manners, *J. Am. Chem. Soc.*, 2005, **127**, 1765–1772.

16 G. R. Whittell, M. D. Hager, U. S. Schubert and I. Manners, *Nat. Mater.*, 2011, **10**, 176–188.

17 L. Friebe, K. Liu, B. Obermeier, S. Petrov, P. Dube and I. Manners, *Chem. Mater.*, 2007, **19**, 2630–2640.

18 Z. M. Al-Badri, R. R. Maddikeri, Y. Zha, H. D. Thaker, P. Dobriyal, R. Shunmugam, T. P. Russell and G. N. Tew, *Nat. Commun.*, 2011, **2**, 482.

19 A. Voevodin, L. M. Campos and X. Roy, *J. Am. Chem. Soc.*, 2018, **140**, 5607–5611.

20 B. Xu, M. Lu, J. Kang, D. Wang, J. Brown and Z. Peng, *Chem. Mater.*, 2005, **17**, 2841–2851.

21 A. Dolbecq, E. Dumas, C. R. Mayer and P. Mialane, *Chem. Rev.*, 2010, **110**, 6009–6048.

22 B. Moraru, N. Hüsing, G. Kickelbick, U. Schubert, P. Fratzl and H. Peterlik, *Chem. Mater.*, 2002, **14**, 2732–2740.

23 D. Hoebbel, I. Pitsch, D. Heidemann, H. Jancke and W. Hiller, *Z. Anorg. Allg. Chem.*, 1990, **583**, 133–144.

24 A. Sellinger and R. M. Laine, *Macromolecules*, 1996, **29**, 2327–2330.

25 X.-H. Zheng, J.-F. Zhao, T.-P. Zhao, T. Yang, X.-K. Ren, C.-Y. Liu, S. Yang and E.-Q. Chen, *Macromolecules*, 2018, **51**, 4484–4493.

26 H. Shi, J. Yang, M. You, Z. Li and C. He, *ACS Mater. Lett.*, 2020, **2**, 296–316.

27 X. Wei, P. J. Carroll and L. G. Sneddon, *Organometallics*, 2004, **23**, 163–165.

28 X. Zhang, L. M. Rendina and M. Müllner, *ACS Polym. Au*, 2024, **4**, 7–33.

29 J. Yan, W. Yang, Q. Zhang and Y. Yan, *Chem. Commun.*, 2020, **56**, 11720–11734.

30 M. S. Messina, C. T. Graefe, P. Chong, O. M. Ebrahim, R. S. Pathuri, N. A. Bernier, H. A. Mills, A. L. Rheingold, R. R. Frontiera, H. D. Maynard and A. M. Spokoyny, *Polym. Chem.*, 2019, **10**, 1660–1667.

31 J. Bedard, T. G. Linford-Wood, B. C. Thompson, U. Werner-Zwanziger, K. M. Marczenko, R. A. Musgrave and S. S. Chitnis, *J. Am. Chem. Soc.*, 2023, **145**, 7569–7579.

32 J. Bedard and S. S. Chitnis, *Chem. Mater.*, 2023, **35**, 8338–8352.

33 M. F. Abdollahi, E. N. Welsh, M. Shayan, A. Olivier, N. Wilson-Faubert, U. Werner-Zwanziger, A. Nazemi, A. Laventure and S. S. Chitnis, *J. Am. Chem. Soc.*, 2025, **147**, 9229–9241.

34 M. Shayan, M. F. Abdollahi, M. C. Lawrence, E. C. Guinand, M. Goulet, T. George, J. D. Masuda, M. J. Katz, A. Laventure, U. Werner-Zwanziger and S. S. Chitnis, *Chem. Commun.*, 2024, **60**, 2629–2632.

35 J. Bedard, N. J. Roberts, M. Shayan, K. L. Bamford, U. Werner-Zwanziger, K. M. Marczenko and S. S. Chitnis, *Angew. Chem., Int. Ed.*, 2022, **61**, e202204851.

36 U. Schubert, *Chem. Mater.*, 2001, **13**, 3487–3494.

37 U. Schubert, *Chem. Soc. Rev.*, 2011, **40**, 575–582.

38 F. Vidal and F. Jäkle, *Angew. Chem., Int. Ed.*, 2019, **58**, 5846–5870.

39 R. D. Miller and J. Michl, *Chem. Rev.*, 1989, **89**, 1359–1410.

40 F. S. Kipping, *J. Chem. Soc.*, 1924, **125**, 2291–2297.

41 E. M. Press, E. A. Marro, S. K. Surampudi, M. A. Siegler, J. A. Tang and R. S. Klausen, *Angew. Chem., Int. Ed.*, 2017, **56**, 568–572.

42 E. A. Marro and R. S. Klausen, *Chem. Mater.*, 2019, **31**, 2202–2211.

43 F. Fang, Q. Jiang and R. S. Klausen, *J. Am. Chem. Soc.*, 2022, **144**, 7834–7843.

44 Q. Jiang, S. Wong and R. S. Klausen, *Polym. Chem.*, 2021, **12**, 4785–4794.

45 E. A. Marro, E. M. Press, M. A. Siegler and R. S. Klausen, *J. Am. Chem. Soc.*, 2018, **140**, 5976–5986.

46 Y. Kawakami, H. Toda, M. Higashino and Y. Yamashita, *Polym. J.*, 1988, **20**, 285–292.

47 E. S. Finkelshtein, K. L. Makovetskii, M. L. Gringolts, Y. V. Rogan, T. G. Golenko, L. E. Starannikova, Y. P. Yampolskii, V. P. Shantarovich and T. Suzuki, *Macromolecules*, 2006, **39**, 7022–7029.

48 P. P. Chapala, M. V. Bermeshev, L. E. Starannikova, N. A. Belov, V. E. Ryzhikh, V. P. Shantarovich, V. G. Lakhtin, N. N. Gavrilova, Y. P. Yampolskii and E. S. Finkelshtein, *Macromolecules*, 2015, **48**, 8055–8061.

49 X. Wang, T. J. Wilson, D. Alentiev, M. Gringolts, E. Finkelshtein, M. Bermeshev and B. K. Long, *Polym. Chem.*, 2021, **12**, 2947–2977.

50 Y. P. Yampolskii, E. S. Finkelshtein, K. L. Makovetskii, V. I. Bondar and V. P. Shantarovich, *J. Appl. Polym. Sci.*, 1996, **62**, 349–357.

51 A. I. Wozniak, E. V. Bermesheva, I. L. Borisov, S. A. Rzhevskiy, A. A. Tyutyunov, S. O. Ilyin, M. A. Topchiy, A. F. Asachenko and M. V. Bermeshev, *Polym. Chem.*, 2023, **14**, 5274–5285.

52 S. Kanaoka and R. H. Grubbs, *Macromolecules*, 1995, **28**, 4707–4713.

53 H. Yin, P. Chapala, M. Bermeshev, B. R. Pauw, A. Schönhals and M. Böhning, *ACS Appl. Polym. Mater.*, 2019, **1**, 844–855.

54 T. Katsumata, M. Shiotsuki, F. Sanda and T. Masuda, *Polymer*, 2009, **50**, 1389–1394.

55 P. Shieh, H. V.-T. Nguyen and J. A. Johnson, *Nat. Chem.*, 2019, **11**, 1124–1132.

56 H. Tetsuka, K. Isobe and M. Hagiwara, *Polym. J.*, 2009, **41**, 643–649.

57 H. Tetsuka, M. Hagiwara and S. Kaita, *Polym. J.*, 2011, **43**, 97–100.

58 A. T. Khan and E. Mondal, *Synlett*, 2003, 694–698.

59 P. Gumbley, X. Hu, J. A. Lawrence III and S. W. Thomas III, *Macromol. Rapid Commun.*, 2013, **34**, 1838–1843.

60 E. Carberry and R. West, *J. Am. Chem. Soc.*, 1969, **91**, 5440–5446.

61 C. Marschner, *Eur. J. Inorg. Chem.*, 1998, **1998**, 221–226.

62 M. Zirngast, J. Baumgartner and C. Marschner, *Organometallics*, 2008, **27**, 6472–6478.

63 H. Wakefield, I. Kevlishvili, K. E. Wentz, Y. Yao, T. B. Kouznetsova, S. J. Melvin, E. G. Ambrosius, A. Herzog-Arbeitman, M. A. Siegler, J. A. Johnson, S. L. Craig, H. J. Kulik and R. S. Klausen, *J. Am. Chem. Soc.*, 2023, **145**, 10187–10196.

64 K. E. Wentz, Y. Yao, I. Kevlishvili, T. B. Kouznetsova, B. A. Mediavilla, H. J. Kulik, S. L. Craig and R. S. Klausen, *Macromolecules*, 2023, **56**, 6776–6782.

65 S. Yajima, Y. Hasegawa, J. Hayashi and M. Iimura, *J. Mater. Sci.*, 1978, **13**, 2569–2576.

66 S. K. Shukla, R. K. Tiwari, A. Ranjan, A. K. Saxena and G. N. Mathur, *Thermochim. Acta*, 2004, **424**, 209–217.

67 V. I. Bondar, Y. M. Kukharskii, Y. P. Yampol'skii, E. S. Finkelshtein and K. L. Makovetskii, *J. Polym. Sci., Part B: Polym. Phys.*, 1993, **31**, 1273–1283.

68 A. Wallner, M. Hölbling, J. Baumgartner and C. Marschner, *Silicon Chem.*, 2007, **3**, 175–185.

69 A. Wallner, R. Emanuelsson, J. Baumgartner, C. Marschner and H. Ottosson, *Organometallics*, 2013, **32**, 396–405.

70 C. Marschner, *Organometallics*, 2006, **25**, 2110–2125.

71 B. J. Ackley, K. L. Martin, T. S. Key, C. M. Clarkson, J. J. Bowen, N. D. Posey, J. F. Ponder Jr, Z. D. Apostolov, M. K. Cinibulk, T. L. Pruyn and M. B. Dickerson, *Chem. Rev.*, 2023, **123**, 4188–4236.

72 H. Li, Y. Zhou, Y. Liu, L. Li, Y. Liu and Q. Wang, *Chem. Soc. Rev.*, 2021, **50**, 6369–6400.

73 R. Lu, J. Wang, T. Duan, T.-Y. Hu, G. Hu, Y. Liu, W. Fu, Q. Han, Y. Lu, L. Lu, S.-D. Cheng, Y. Dai, D. Hu, Z. Shen, C.-L. Jia, C. Ma and M. Liu, *Nat. Commun.*, 2024, **15**, 6596.

74 B. Fan, F. Liu, G. Yang, H. Li, G. Zhang, S. Jiang and Q. Wang, *IET Nanodielectr.*, 2018, **1**, 32–40.